

Supplemental material

Fassier et al., <https://doi.org/10.1083/jcb.201604108>

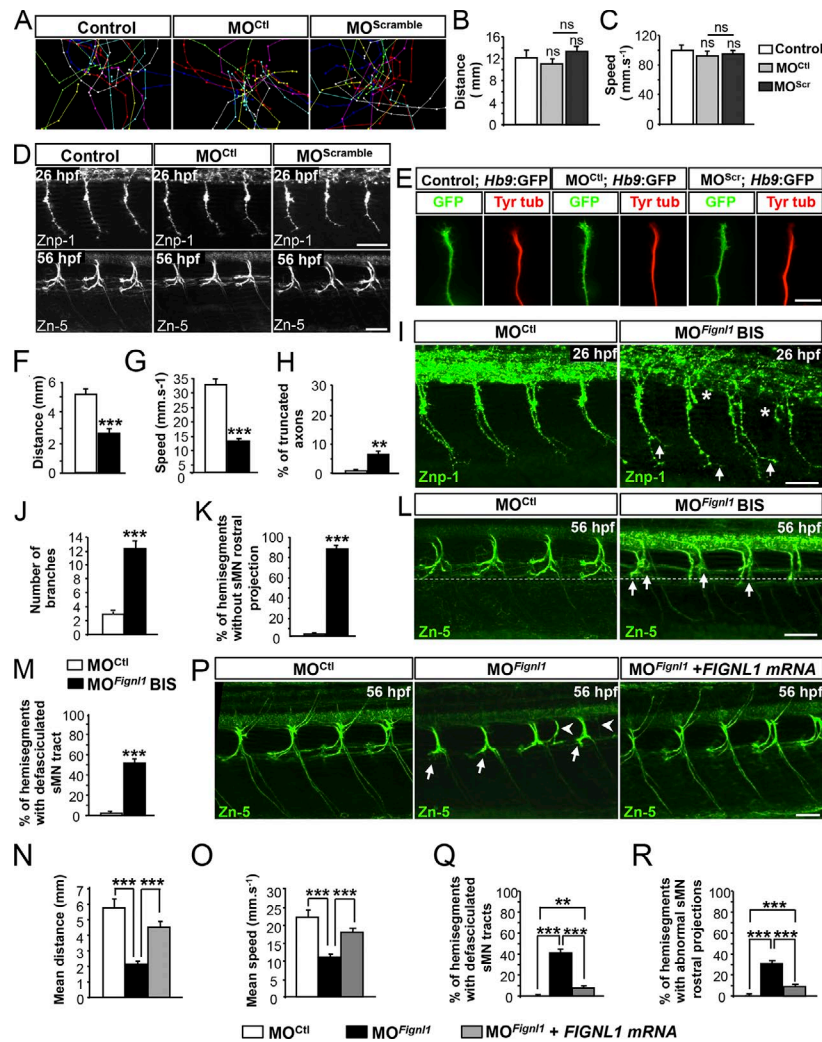


Figure S1. **Morpholinos targeted against *Figl1* mRNA specifically alter motor axon targeting and larval mobility compared with control morpholinos.** (A–C) Analysis of larval mobility using a touch–escape response test. (A) Tracking analysis of noninjected larvae (Control; $n = 24$) and larvae injected with *Figl1*-mismatch (MO^{ctI} ; $n = 25$) or control scramble morpholinos ($MO^{Scramble}$; $n = 24$) at 56 hpf. Each line represents the trajectory of one larva after a touch stimulation. (B and C) Quantifications of the mean swimming distance (B) and velocity (C). (D) Immunolabeling of primary (top) and secondary (bottom) motor neurons in 26- and 56-hpf control, MO^{ctI} , and $MO^{Scramble}$ embryos by using Znp-1 (top) and Zn-5 (bottom) antibodies. Injection of each control morpholino does not affect motor neuron development compared with noninjected control embryos and larvae. Bars, 50 μ m. (E) Primary cultures of SMNs from 24-hpf control, MO^{ctI} , and $MO^{Scramble}$ *Tg(Hb9:GFP)* embryos immunolabeled at 9 hpf with anti-GFP (in green) and tyrosinated-tubulin (in red) antibodies. GC morphology of MO^{ctI} and $MO^{Scramble}$ motor neurons were undistinguishable from control GCs. Bar, 10 μ m. (F and G) Analysis of 56-hpf control ($n = 41$) and $MO^{Figl1}BIS$ -injected ($n = 69$) larval locomotion in a touch–escape response test. (F) Quantification of the mean swimming distance. (G) Quantification of the mean swimming speed. (H–J) Analysis of pMN in 26-hpf control ($n = 17$) and $MO^{Figl1}BIS$ -injected embryos ($n = 21$). (H) Mean percentage of truncated axons. (J) Mean number of branches. (H and J) Quantifications were performed on 12 hemisegments around the yolk tube. (I) Immunostaining of 26-hpf control and $MO^{Figl1}BIS$ -injected embryos by using Znp-1 antibody. Some ventrally projecting CaP axons of $MO^{Figl1}BIS$ -injected embryos appear truncated (asterisks) or show aberrant distal branches (arrows). (K–M) Analysis of sMN in 56-hpf control ($n = 18$) and morphant ($n = 18$) larvae. (K) Mean percentage of hemisegments without sMN rostral projection. (M) Percentage of hemisegments with defasciculated sMN tracts. Quantifications were performed on 24 hemisegments. (L) Immunolabeling of sMN in 56-hpf control and $MO^{Figl1}BIS$ -injected larvae by using Zn-5 antibody. sMN axons of $MO^{Figl1}BIS$ -injected larvae fail to grow rostrally and defasciculate at the horizontal myoseptum (arrows). (N and O) Quantification of the mean covered distance (N) and mean swimming speed (O) of 56-hpf control ($n = 38$), *Figl1* morphant ($n = 100$), and doubly ($MO^{Figl1} + FIGNL1$ -mRNA) injected ($n = 64$) larvae in a touch–escape response test. (P) Immunostaining of sMNs in 56-hpf control ($n = 17$), *Figl1* morphant ($n = 17$), and doubly injected larvae ($MO^{Figl1} + FIGNL1$ -mRNA; $n = 19$) by using Zn-5 antibody. Human *FIGNL1* overexpression partially rescued the abnormal defasciculation of rostral projections (arrows) and the aberrant ectopic sorting (arrowheads) of morphant sMN tracts. Bars, 40 μ m. (D, I, L, and P) Lateral views of the trunk; anterior to the left. n values indicate the total number of embryos analyzed in at least three independent experiments. (Q and R) Percentage of hemisegments with defasciculated sMN tracts (Q) and abnormal sMN rostral projections (R). Quantifications were performed on 24 hemisegments. ns, $P > 0.05$; **, $P \leq 0.01$; ***, $P \leq 0.001$; unpaired two-tailed t test. Error bars are SEM.

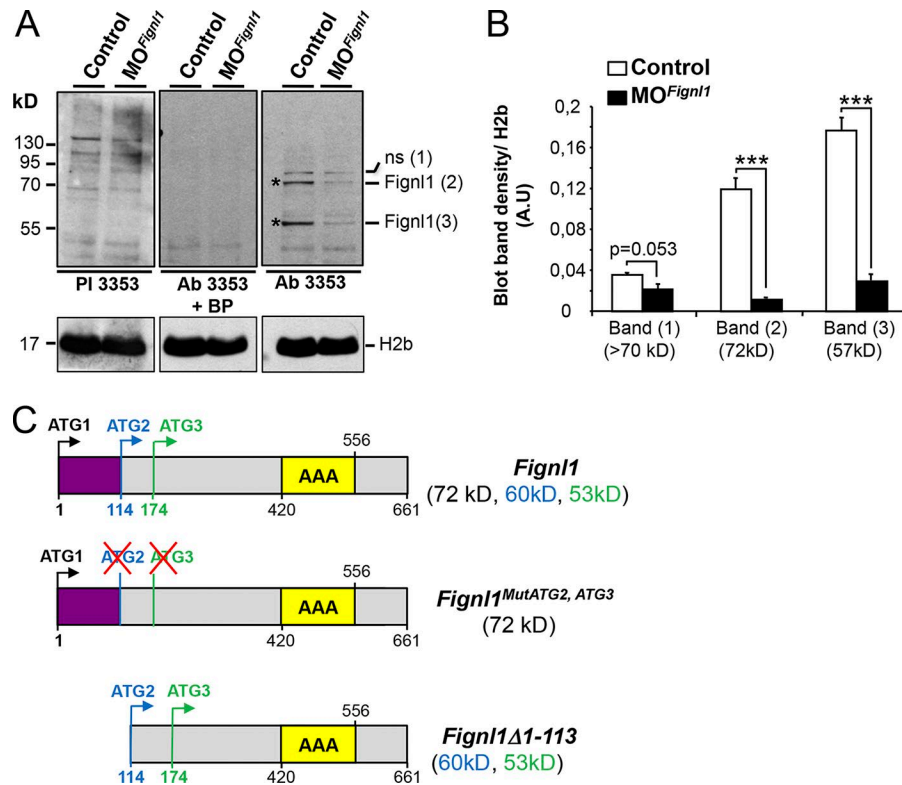


Figure S2. **Figl1 isoforms and knockdown efficiency.** (A) WB analysis of total protein extracts from 28-hpf control and MO^{Figl1}-injected embryos using preimmune serum (PI 3353; left) or affinity-purified Figl1 polyclonal antibody (Ab 3353) preincubated or not with the blocking peptide (BP; middle and right, respectively). A ratio antibody/blocking peptide of 1:10 was used. Figl1 antibody reproducibly recognized two bands at 72 (Figl1, band 2) and 57 kD (Figl1, band 3) that (a) were absent from the blot with PI 3353, (b) disappeared after preincubation with the blocking peptide, and (c) were both strikingly reduced in morphant embryos. The 72- and 57-kD bands correspond with the predictive molecular weight of zebrafish full-length FL-Figl1 and to an apparent shorter isoform, which may correspond with a shorter isoform translated from a second in-frame ATG codon (methionine 114). The fainter 85-kD band, which was also detected by our Figl1 antibody and disappeared after preincubation with the blocking peptide, is most likely a nonspecific band (ns; band 1) because its expression was not affected by Figl1 morpholinos. H2b was used as a loading control. (B) Quantification of bands 1–3 density normalized to H2b values from three independent experiments. ***, $P \leq 0.001$; unpaired two-tailed t test. Error bars are SEM. (C) Schematic representation of the different constructs used to study the alternative translation of Figl1 transcript. The full-length zebrafish Figl1 cDNA (FL-Figl1 construct) contains three in-frame ATG codons corresponding with methionine 1 (ATG1; black), 114 (ATG2; blue), and 174 (ATG3; green). Targeted mutagenesis of the ATG2 and ATG3 codons (FL-Figl1^{MutATG2, ATG3}) were carried out to assess whether alternative translation from these initiation codons generates N-terminally truncated isoforms. Figl1 cDNA was also cloned from the second ATG to produce only N-terminally truncated isoforms (Figl1Δ1–113). Predictive molecular weights of the different Figl1 isoforms are indicated in brackets. WB analyses of Figl1 isoforms synthesized from these constructs are presented in Fig. 3.

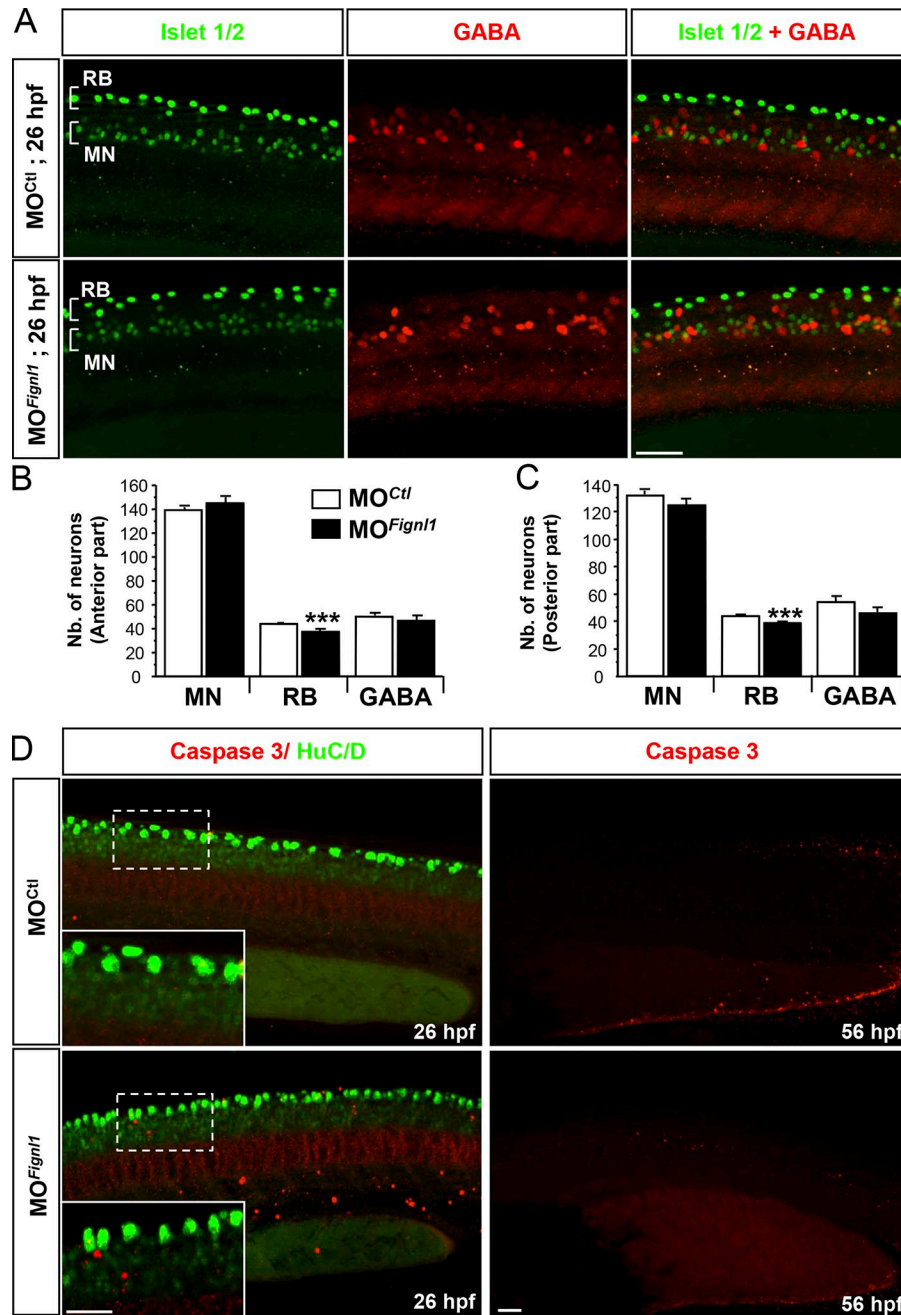


Figure S3. **Figl1** depletion does not perturb the specification, localization, or survival of SMNs. **(A)** Immunolabeling of SMNs (MNs), RB sensory neurons, and GABAergic interneurons in 26-hpf MO^{Ctl} and MO^{Figl1} embryos with Islet1/2 (green) and GABA (red) antibodies. Lateral views of the trunk; anterior is to the left. Bar, 50 μ m. **(B and C)** Mean number (Nb.) of MNs, RB neurons, and GABAergic interneurons (GABA). Quantifications were performed on 26-hpf control ($n = 22$) and morphant ($n = 21$) embryos pooled from three independent experiments. 12 hemisegments were analyzed in the anterior (B) and posterior regions (C) of each embryonic trunk. ***, $P \leq 0.001$; unpaired two-tailed t test. Error bars are SEM. **(D)** Immunolabeling of activated caspase 3 (red) and the neuronal postmitotic marker HuC/D (green; left) or caspase 3 alone (red; right) in 26- (left) or 56-hpf (right) MO^{Ctl} and MO^{Figl1} embryos and larvae. Insets represent higher magnifications of the indicated boxed regions. *Figl1* knockdown does not induce apoptotic cell death of spinal neurons. Bars, 30 μ m.

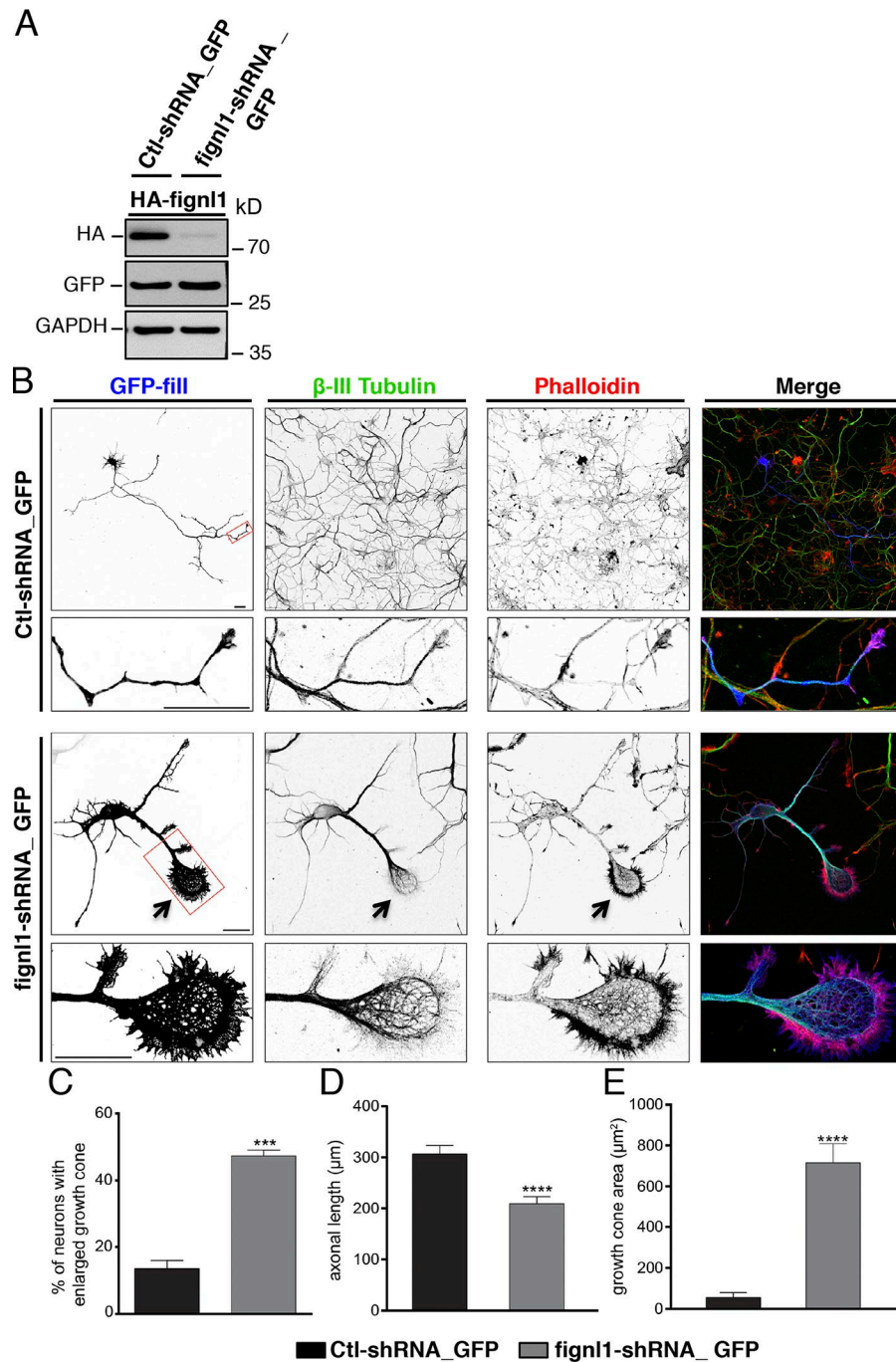


Figure S4. **Knockdown of *figl1* in cultured mammalian neurons affects GC morphology and MT organization as in zebrafish neurons.** (A) Knockdown efficiency of Figl1-shRNA. WB analysis of protein extracts from COS-7 cells cotransfected with mouse HA-Figl1^{3'UTR} and control-shRNA_GFP or 3'UTR-targeted Figl1-shRNA_GFP (cloned in pSUPER.neo + GFP vectors) by using HA, GFP, and GAPDH antibodies. GFP and GAPDH were used as transfection and loading controls, respectively. HA-Figl1 expression is strikingly reduced by Figl1-shRNA. (B) Cultured hippocampal neurons transfected at DIV1 with control-shRNA_GFP or Figl1-shRNA_GFP and stained at DIV3 for GFP, β -III tubulin, and F-actin (phalloidin). Bottom panels are higher magnifications of the corresponding boxed region. Arrows indicate enlarged GCs of Figl1-shRNA transfected neurons. Bars, 30 μ m. (C) Mean percentage of transfected neurons with enlarged GCs. Quantifications were carried out on at least 150 transfected neurons per condition in three independent experiments. (D) Mean axonal length. (E) Mean GC area. Quantifications were performed on 32 control-shRNA_GFP- and 33 Figl1-shRNA-GFP-transfected neurons collected from three independent experiments. ***, $P \leq 0.001$; ****, $P \leq 0.0001$; unpaired two-tailed t test. Error bars are SEM.

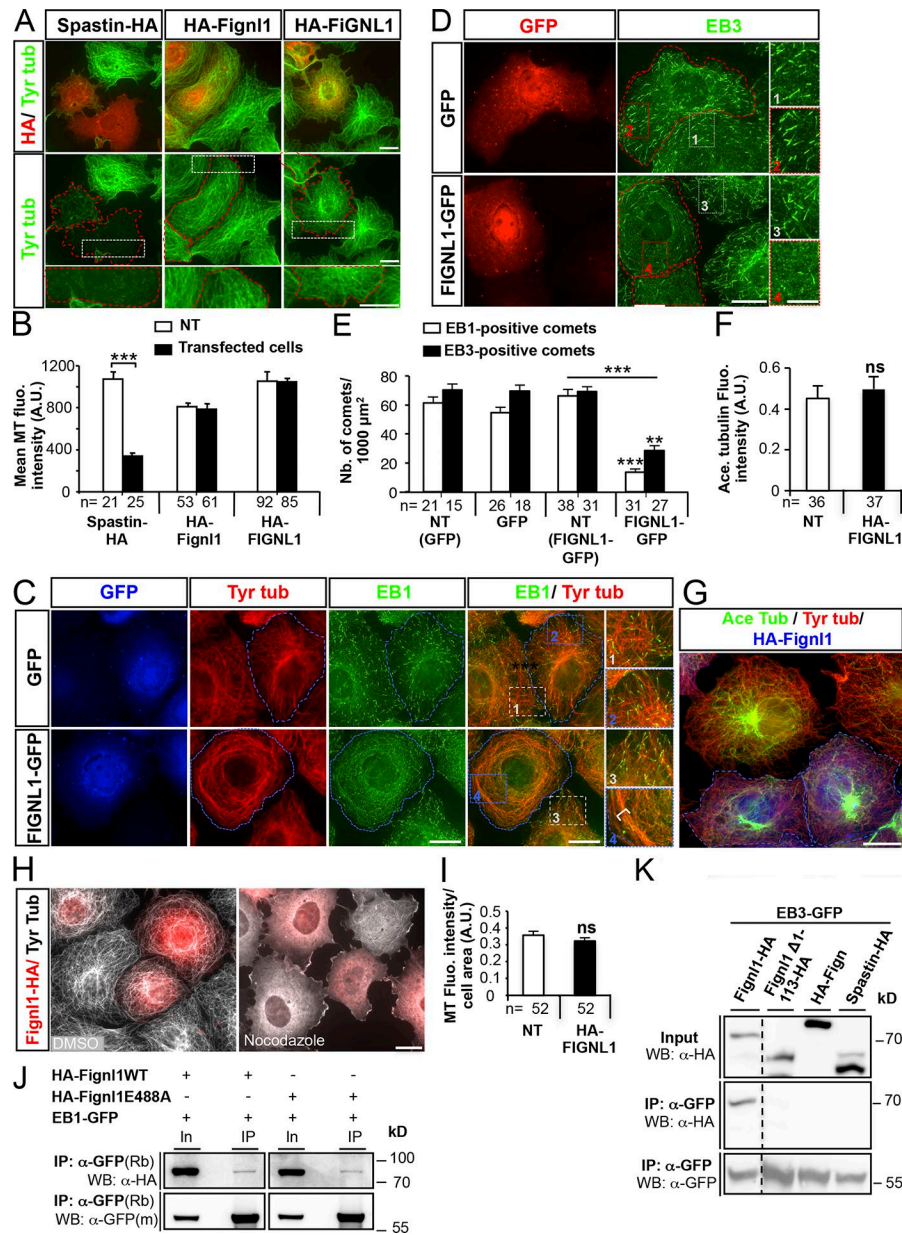
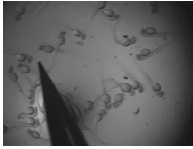


Figure S5. **Fignl1** overexpression displaces +TIPs from MT plus ends through its specific interaction with EB1/3. **(A)** Overexpression of HA-tagged zebrafish spastin (spastin-HA), zebrafish Fignl1 (HA-Fignl1), and human fignl1 (HA-FIGNL1) in COS-7 cells and immunolabeling with HA (red) and tyrosinated tubulin (green) antibodies 24 hpt. Transfected cells are delineated by red dashed lines. Bottom panels represent higher magnifications of boxed regions in corresponding panels. **(B)** Mean MT fluorescence intensity related to cell area. **(C and D)** Overexpression of GFP-tagged human FIGNL1 (FIGNL1-GFP) or GFP alone (GFP) in COS-7 cells followed by immunolabeling by using GFP (C, blue), EB1 (C, green), and tyrosinated tubulin (C, red) antibodies or GFP (D, red) and EB3 (D, green) antibodies at 24 hpt. Transfected cells are delineated by blue (C) or red (D) dotted lines. Right panels represent higher magnifications of the indicated boxed region on adjacent left panels. **(E)** Mean number of EB1- and EB3-positive comets per 1,000 μm^2 . **(F and G)** COS-7 cells transfected with HA-Fignl1 and immunolabeled with HA, acetylated (Ace Tubulin), and tyrosinated tubulin (Tyr tubulin) antibodies. **(F)** Mean acetylated tubulin fluorescence intensity related to cell area. **(G)** Transfected cells are delineated by blue dashed lines. **(H)** COS-7 cells transfected with HA-Fignl1 were treated 24 hpt with 20 μM nocodazole for 15 min or with DMSO as a control and stained with HA and tyrosinated tubulin antibodies. Bars: (A, C and D [main images], F, and H) 20 μm ; (C and D, insets) 10 μm . **(I)** Mean MT fluorescence intensity related to cell area. NT, nontransfected. The total number of cells (n) analyzed per condition in three independent experiments is mentioned under the corresponding histogram bar. **, $P \leq 0.01$; ***, $P \leq 0.001$; unpaired two-tailed t test. Error bars are SEM. **(J)** Co-IP of HA-Fignl1 or mutated HA-Fignl1E488A with EB1-GFP. COS-7 cells cotransfected with EB1-GFP and HA-Fignl1 or HA-Fignl1E488A were lysed in RIPA buffer 24 hpt. Co-IP assays were performed with a GFP antibody, and immunoprecipitated (IP) proteins were revealed by WB using HA or GFP antibodies. WT and ATP hydrolysis-deficient zebrafish Fignl1 equally coimmunoprecipitate with the core +TIP EB1. **(K)** co-IP of HA-tagged Fignl1 isoforms and their homologues Fign and spastin with EB3-GFP. COS-7 cells were cotransfected with EB3-GFP and FL-Fignl1-HA, Fignl1 Δ 113-HA, HA-Fign, or spastin-HA. Co-IP assays were performed 24 hpt with a GFP antibody, and immunoprecipitated proteins were revealed using either HA or GFP antibody. m: mouse; Rb, rabbit.



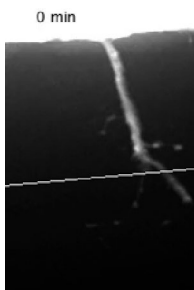
Video 1. **The swimming deficit of *Figl1* morphant is partially rescued by misexpression of human *FIGNL1*.** Touch-evoked mobility of 56-hpf control larvae. Images were acquired under a binocular stereomicroscope with a Canon Power Shot A520 camera. Frames were taken every 0.07 s. Playback speed: 15 frames per second.



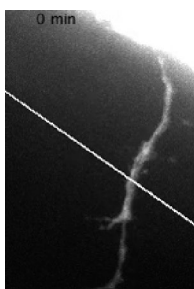
Video 2. **The swimming deficit of *Figl1* morphant is partially rescued by misexpression of human *FIGNL1*.** Touch-evoked mobility of MO^{Figl1}-injected larvae. Images were acquired under a binocular stereomicroscope with a Canon Power Shot A520 camera. Frames were taken every 0.07 s. Playback speed: 15 frames per second.



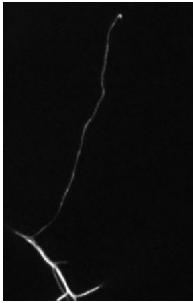
Video 3. **The swimming deficit of *Figl1* morphant is partially rescued by misexpression of human *FIGNL1*.** Touch-evoked mobility of doubly (MO^{Figl1} + *FIGNL1*-mRNA) injected larvae. Images were acquired under a binocular stereomicroscope with a Canon Power Shot A520 camera. Frames were taken every 0.07 s. Playback speed: 15 frames per second.



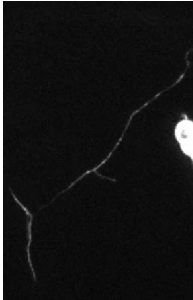
Video 4. ***Figl1* knockdown dramatically alters spinal motor axon pathfinding.** Time-lapse videomicroscopy on control Tg(*Olig2*:GFP) larvae from 42 to 76 hpf using a spinning-disk microscope. The white line indicates the horizontal myoseptum. Frames were taken every 8 min. Playback speed: seven frames per second.



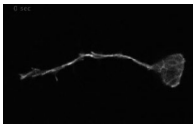
Video 5. ***Figl1* knockdown dramatically alters spinal motor axon pathfinding.** Time-lapse videomicroscopy on MO^{Figl1}-injected Tg(*Olig2*:GFP) larvae from 42 to 76 hpf using a spinning-disk microscope. The white line indicates the horizontal myoseptum. Frames were taken every 8 min. Playback speed: seven frames per second.



Video 6. **Figl1 depletion increases MT growth rate and duration in spinal motor axons.** Time-lapse videomicroscopy recordings of EB3-GFP comets in spinal motor axons of 52-hpf control larvae using a spinning disk microscope. Frames were taken every 4 s. Playback speed: 15 frames per second.



Video 7. **Figl1 depletion increases MT growth rate and duration in spinal motor axons.** Time-lapse videomicroscopy recordings of EB3-GFP comets in spinal motor axons of MO^{Figl1}-injected larvae by using a spinning-disk microscope. Frames were taken every 4 s. Playback speed: 15 frames per second.



Video 8. **Figl1 knockdown alters MT dynamics and growth directionality in spinal motor GCs.** Time-lapse videomicroscopy recordings of EB3-GFP comets in primary cultures of SMNs from 24-hpf control Tg(*Hb9*:Gal4; UAS:EB3-GFP) embryos. Frames were acquired with a spinning-disk microscope every 2 s. Playback speed: 15 frames per second.



Video 9. **Figl1 knockdown alters MT dynamics and growth directionality in spinal motor GCs.** Time-lapse videomicroscopy recordings of EB3-GFP comets in primary cultures of SMNs from *Figl1* morphant Tg(*Hb9*:Gal4; UAS:EB3-GFP) embryos. Frames were acquired with a spinning-disk microscope every 2 s. Playback speed: 15 frames per second.